

Social Regulation of the Electrical Properties of Gonadotropin-Releasing Hormone Neurons in a Cichlid Fish (*Astatotilapia burtoni*)¹

Anna K. Greenwood² and Russell D. Fernald

Program in Neuroscience, Stanford University, Stanford, California 94305

ABSTRACT

Variation in reproductive capacity is common across the lives of all animals. In vertebrates, hypothalamic neurons that secrete GnRH are a primary mediator of such reproductive plasticity. Since social interactions suppress gonadal maturity in the African cichlid fish, *Astatotilapia (Haplochromis) burtoni*, we investigated whether the electrical properties of GnRH neurons were also socially regulated. Adult *A. burtoni* males are either territorial (T) and reproductively active or nonterritorial (NT) and reproductively regressed, depending upon their social environment. We compared the basic electrical properties of hypothalamic GnRH neurons from T and NT males using whole-cell electrophysiology in vitro. GnRH neurons were spontaneously active and exhibited several different activity patterns. A small fraction of neurons exhibited episodic activity patterns, which have been described in GnRH neurons from mammals. The type of activity pattern and spontaneous firing rate did not vary with reproductive capacity; however, several basic electrical properties were different. Neurons from T males were larger than those from NT males and had higher membrane capacitance and lower input resistance. In neurons from NT males, action potential duration was significantly longer and after-hyperpolarization characteristics were diminished, which led to a tendency for neurons from NT males to fire less rapidly in response to current injection. We predict this could serve to decrease GnRH release in NT males. These data are the first electrophysiological characterization of hypothalamic GnRH neurons in a nonmammalian species and provide evidence for several changes in electrical properties with reproductive state.

behavior, gonadotropin-releasing hormone, neuroendocrinology

INTRODUCTION

Social influences on reproductive capacity have been identified in species ranging from insects to humans [e.g., 1, 2]. In vertebrates, interactions between conspecifics can either stimulate or suppress fertility by modulating the main reproductive control system, the hypothalamic-pituitary-gonadal (HPG) axis [3–5]. Hypothalamic GnRH neurons are at the apex of HPG axis control and hence are a prime site for regulation of reproductive physiology [6–9], including regulation by social cues [10, 11].

Social encounters between adult males of the African cichlid fish *Astatotilapia* (formerly *Haplochromis*) *burtoni*

induce specific changes in the structure and function of GnRH neurons, making this an excellent model for understanding the neural basis of alterations in reproductive capacity [12–14]. In their native habitat, *A. burtoni* males compete for a limited number of territories that provide them access to food and a refuge for mating [15, 16]. Consequently, adult *A. burtoni* males exist in one of two social states: territorial (T) or nonterritorial (NT). Successful T males defend territories, are brightly colored, act aggressively toward other males, and solicit and court females for spawning [13, 15]. In contrast, NT males, which cannot successfully compete for territories, are cryptically colored, school with females, and do not perform aggressive or courtship behaviors [13, 17]. The NT state results from social suppression. In the absence of competition, all males will develop into T males; however, in normal community settings, the development of most juvenile males into reproductively mature adults is suppressed as a result of aggressive attacks by larger T males [12, 17]. In addition, adult T males can be socially suppressed by encounters with larger males, causing them to revert to an NT state [13, 14]. In fact, depending upon the social environment, males can switch social status repeatedly during their lives [18].

In addition to differences in behavior and appearance, the reproductive capacity of *A. burtoni* males is linked to their social state. Most overtly, T males have large gonads containing mature sperm, whereas NT males have small gonads containing mostly sperm precursors [13, 17]. Additionally, T males have higher levels of circulating androgens (unpublished data) [19]. These peripheral differences in the reproductive system are regulated by differences in GnRH neurons in the hypothalamus: GnRH neurons in T males are larger and synthesize more GnRH than those in NT males [12–14]. Each time a male changes social status, his HPG axis transforms to match his new social rank [13, 14].

Given the dramatic plasticity in the size and hormone production of GnRH neurons in *A. burtoni* males, and the essential role of GnRH neurons in controlling the fate of the gonads, we wondered whether the functional output of *A. burtoni* GnRH neurons might also change with social and reproductive status. Specifically, since GnRH, like other neurohormones, is released via action potentials [20], we hypothesized that there would be identifiable changes in the electrical properties of GnRH neurons of T and NT males related to differences in their HPG axis maturity. There is precedent for such a hypothesis, since in other neuroendocrine systems there are well-described changes in electrical properties with long-term changes in endocrine demands [e.g., 21].

Although previous work has provided a good electrophysiological characterization of adult mammalian GnRH neurons [22–25], in fish the only GnRH neurons that have

¹Supported by a NINDS 34950/Javits award to R.D.F.

²Correspondence: Anna K. Greenwood, Jordan Hall, Building 420, Stanford University, Stanford, CA 94305-2130. FAX: 650 723 0881; e-mail: akg@stanfordalumni.org

Received: 23 March 2004.

First decision: 13 April 2004.

Accepted: 10 May 2004.

© 2004 by the Society for the Study of Reproduction, Inc.

ISSN: 0006-3363. <http://www.biolreprod.org>

thus far been electrically characterized are a nonhypothalamic population located in the terminal nerve, which expresses a form of GnRH that does not act in the reproductive axis [26, 27]. To our knowledge, the electrical properties of hypothalamic GnRH neurons have not been described in any nonmammal. The goal of this study was to characterize the electrical properties of fish preoptic area GnRH neurons using whole-cell electrophysiology and to compare these properties in reproductive (T) and nonreproductive (NT) animals.

MATERIALS AND METHODS

Animals

Astatotilapia burtoni were bred in the laboratory from a population derived from wild-caught stock [15, 16]. All animals were treated in accordance with regulations of the Stanford University Administrative Panel on Laboratory Animal Care. Animals were maintained in aquaria (85 × 56 × 32 cm) in water treated to match their native environment (pH 8.0, 28°C). Aquaria received full-spectrum lighting (12L:12D) with an additional 10 min of “twilight” in morning and evening. Fish were fed each morning (Cichlid flakes and pellets; Aquadine, Healdsburg, CA). Animals were housed in communities containing 6–12 males and 6–12 females. All males were identified with individualized tags and observed at least once per week to determine their social status. Social status was determined by observation of body color patterns and the performance of state-specific behaviors, including the tendency to school or defend a territory [13, 15]. Body weight and standard length (nose to base of tail) were taken at the time they were killed. Gonads were removed and the gonadosomatic index was calculated (gonad weight/body weight × 100) to characterize reproductive status.

Tissue Preparation

Two to three hours after the lights were turned on, fish were caught and quickly decapitated. Brains were removed and placed in ice-cold artificial cerebrospinal fluid (ACSF) saturated with 95% oxygen and 5% carbon dioxide to a final pH of 7.4. ACSF contained 127 mM sodium chloride, 1.9 mM potassium chloride, 1.2 mM monobasic potassium phosphate, 2.4 mM calcium chloride, 1.3 mM magnesium sulfate, 26 mM sodium bicarbonate, and 25 mM glucose and was adjusted to 315 mOsm. Two types of recording preparations were utilized: brain slice and whole brain in vitro. To prepare slices, the brain was dissected to remove meningeal layers, and the optic nerves, which in fish are completely crossed and enter the brain in one nerve bundle per hemisphere, were trimmed flush with the brain. The brain was then embedded in low-melting agarose composed of 4.25% NuSieve agarose (BioWittaker Molecular Applications, Rockland, ME) and 2.25% LMP agarose (Invitrogen, Carlsbad, CA) in ACSF. The agarose-brain block was affixed to a vibratome chamber with cyanoacrylate glue, and vibratome sections of 250 μm were cut at an angle parallel to the ventral surface of the telencephalic lobes (see Fig. 1). Slices were then transferred into an incubation chamber containing ice-cold ACSF where they remained for at least 1 h while the bath solution slowly warmed to room temperature (23°–26°C). Before recording, slices were transferred to a recording chamber and were stabilized using a “slice keeper” (Warner Instruments, Hamden, CT). For recordings from the whole brain, the brain was removed and placed into ice-cold ACSF where it rested for at least 1 h. The brain was then pinned upside down in a Sylgard-filled recording chamber using thin stainless steel insect pins through the spinal cord, tectal lobes, anterior telencephalon, and optic nerves. Meningeal layers were removed for access to the tissue.

Electrophysiology

Tissue was continuously perfused with room-temperature ACSF saturated with 95% oxygen and 5% carbon dioxide. Cells were visualized using a 40× immersion objective on an upright fixed-stage microscope (Axioscope; Carl Zeiss, Oberkochen, Germany) and an infrared camera (C2400, Hamamatsu, Shizuoka, Japan) connected to a monochrome monitor (Sony, New York, New York). Patch pipettes were pulled from thin-walled borosilicate glass capillaries (OD 1.5, ID 1.1; Sutter Instruments, Novato, CA) using a Flaming-Brown pipette puller (P-97; Sutter Instruments) to a bubble number of 5.4 [28]. The final electrode resistance was 8 MΩ. Intracellular electrode solution components were 130 mM potassium gluconate, 10 mM EGTA, 30 mM potassium hydroxide, 10 mM

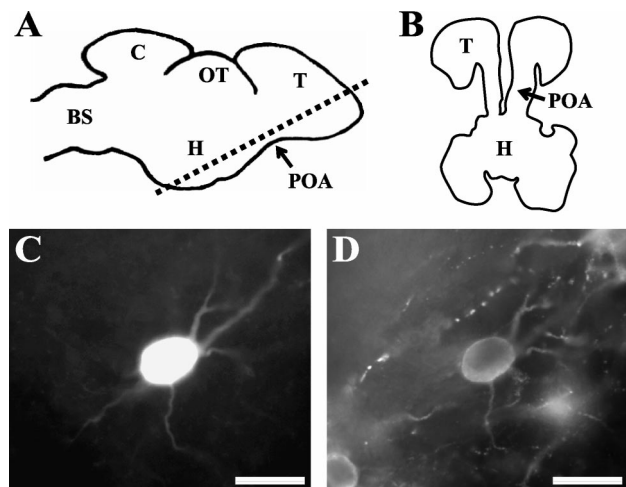


FIG. 1. Depiction of slice preparation and post hoc identification of GnRH neurons. **A**) Schematic illustration of the brain with a dashed line indicating the angle at which vibratome slices used for electrophysiology were prepared. BS, Brainstem; C, cerebellum; H, hypothalamus; OT, optic tectum; POA, preoptic area; T, telencephalon. **B**) Illustration of a typical vibratome slice. Fluorescent photomicrographs of the same GnRH neuron are shown in **(C)** and **(D)**. **C**) Detection of neurobiotin tracer injected during recording. **D**) Immunoreactivity for GnRH. Bar = 20 μm.

HEPES, 2 mM magnesium-ATP salt, 1 mM magnesium chloride, 1 mM sodium hydroxide; solution was pH 7.3 and was adjusted to 290–295 mOsm. To allow for post hoc identification of the cells, the intracellular solution also contained 5 mM neurobiotin tracer (Vector Laboratories, Burlingame, CA). Intracellular solution was filtered through a 0.2 μm filter immediately before use. A liquid junction potential of 10 mV was calculated, and this value has been subtracted from reported recordings. Electrodes were positioned using a motorized micromanipulator (MP-225; Sutter Instruments). Whole-cell current-clamp recordings were obtained using the bridge mode of an amplifier (Axoclamp 2B; Axon Instruments, Union City, CA). Bridge balance was adjusted to compensate for any access resistance. Recordings were terminated if access resistance was larger than 20 MΩ or changed substantially over time. Traces were amplified using a preamplifier (Brownlee Precision Instruments, San Jose, CA) and then digitized at 10 kHz (Digidata 1200; Axon Instruments) and captured on a computer using acquisition software (pClamp 8 and 9; Axon Instruments).

Cell Targeting and Verification of Cell Identity

Neurons were targeted for recording based on their anatomical location and their size relative to other adjacent neurons. In fish, GnRH neurons are clustered in a distinct nucleus, the magnocellular portion of the anterior parvocellular preoptic nucleus (aPPn) [29], an anatomy quite unlike their diffuse distribution across several nuclei in tetrapods [12, 29, 30]. GnRH neurons are the only large neuroendocrine cells in this area, and in both T and NT brains they are substantially larger than neighboring cells such as glia and interneurons. In our slice preparation (see Fig. 1), GnRH neurons were clustered within several hundred microns of the medial edge of the telencephalic lobe, and the population was bordered by the preoptic-hypophysial tract on the lateral edge and by the anterior commissure more rostrally.

In both brain slices and the whole brain preparation, the anatomy of the aPPn was easily distinguished and the prominent GnRH neurons were readily identified. However, to verify that recorded cells were indeed GnRH neurons, cells were labeled with neurobiotin tracer (see above) during recording and the tissue was processed for GnRH immunohistochemistry. Cells were dye-filled after the investigation of basic properties was complete using 500 ms pulses of 50 pA of positive current at 1 Hz for approximately 5 min. Slices were fixed for 1–2 h in 4% paraformaldehyde in PBS, and whole brains were fixed overnight at 4°C. Slices were then washed in PBS and stored in PBS at 4°C until immunohistochemistry was performed (up to 2 wk). Whole brains were embedded in agarose and sliced at 250 μm on a vibratome before processing. GnRH neurons were identified using a primary antibody raised against mammalian GnRH (H. Urbanski, Oregon Health Sciences University, Portland, OR). This antibody (HU4H) has been determined to have low cross-reactivity with the form of GnRH found in the terminal nerve of fishes (H. Urbanski, personal

communication). Immunohistochemistry was performed on free-floating sections with steps as follows: tissue was incubated for at least 2 h in PBT buffer (PBS containing 0.2% BSA and 0.1% Triton-X) containing 10% normal goat serum (Pel-Freez, Rogers, AR); incubated overnight at 4°C in primary anti-GnRH antibody diluted 1000-fold in PBT with 10% normal goat serum; washed four times for at least 15 min each in PBT buffer; incubated for at least 2 h in a secondary antibody mix containing avidin-Texas red and anti-mouse fluorescein each diluted 1:500 in PBT or PBS (both secondary antibodies from Vector Laboratories); washed several times in PBS; and coverslipped (Fluoromount G mounting media; Southern Biotechnology Association, Birmingham, AL).

We used a standard fluorescence microscope (Axioscope; Zeiss) to determine whether neurobiotin-filled neurons contained GnRH immunoreactivity. Images of neurobiotin and GnRH signals were captured using a camera attached to a computer (SPOT camera; Diagnostic Instruments, Sterling Heights, MI). An example of a GnRH-positive, neurobiotin-filled neuron is shown in Figure 1. During the optimization of the recording procedure and subsequent experimental recordings included in this report, 101 neurons were filled with neurobiotin, and 93 (92%) of these were GnRH positive. Most of the cells that lacked GnRH immunoreactivity were located more deeply within slices, suggesting that antibody penetration may have been limited in these particular cells (data not shown). This high rate of successful identification led us to be confident in our ability to identify GnRH neurons using anatomical criteria, and therefore we included some cells in our analysis that we were not able to positively identify immunohistochemically for various reasons (e.g., cell not effectively labeled with neurobiotin, tissue lost or damaged during immunohistochemistry; see below for sample size), but which in every other way resembled GnRH neurons (e.g., anatomy and electrical properties). Of the 33 neurons that reached our electrical criteria (see below), eight (NT, 2; T, 6) were not immuno-identified. No electrical properties were significantly different as a function of whether or not the cell had been immuno-identified (data not shown).

To examine differences in cell size as a function of social status, we determined the cross-sectional area for each filled cell by measuring the neurobiotin-filled cell body profile (NIH Image; NIH, Bethesda, MD) [12, 13].

Analysis of Electrical Properties

An array of basic electrical properties was measured in order to characterize the properties of *A. burtoni* GnRH neurons. Neurons included for analysis had overshooting action potentials greater than 65 mV (baseline to peak) and a resting membrane potential (RMP) more negative than -50 mV that did not vary substantially (<5 mV) throughout the recording. These criteria were chosen because they provided a quantitative way to select neurons that qualitatively appeared to be electrically healthy and intact. Thirty-three neurons (NT, 13; T, 20) reached these criteria and were included in this analysis (see Results). For consistency, spontaneous firing rate was measured within the first 20 sec of whole-cell penetration and is designated "initial" firing rate. Action potential parameters (duration, height, rise time, and decay time) were averaged from traces of spontaneous activity (event detection search parameters, Clampfit 9; Axon Instruments). Cells that were silent ($n = 3$; see Results) were injected with small amounts of positive current to induce action potentials for analysis. Action potential duration was determined at half-height measured from baseline (RMP) to peak. The peak depth of the after-hyperpolarization (AHP) and the time of the AHP peak were determined from the same traces of spontaneous activity (event detection search parameters, Clampfit 9; Axon Instruments). The threshold was the potential at which the first derivative of the voltage trace was increasing by 1 V/sec.

Evoked membrane properties were determined from a series of current steps. Cells were presented with 500 ms current steps of 10 pA from -50 to +50 pA and/or 50 pA steps from -250 to +250 pA, depending on input resistance. In order to compare passive and evoked properties between cells, we compared a set membrane potential change (approximately 20 mV from rest) instead of a given current step because neurons had varied input resistances depending upon cell size (see Results). The input resistance and membrane time constant were determined using a hyperpolarizing current step, that caused an approximately 20 mV change in potential. The membrane time constant was determined by fitting a single exponential to the charging curve (Clampfit; Axon Instruments). The discharge was not used because some cells displayed a rebound spike following hyperpolarization. Total membrane capacitance was calculated using the equation $\tau = RC$, where τ = time constant, R = resistance, and C = capacitance. Evoked firing properties including interspike interval and accommodation were measured by comparing spiking in response to positive

TABLE 1. Cell size-related properties as a function of reproductive state.*

	Nonterritorial (NT) males	Territorial (T) males
Cross-sectional area (μm^2)	228 \pm 48 [†]	350 \pm 90
Input resistance (m Ω)	656 \pm 430 [†]	343 \pm 177
Capacitance (pF)	125 \pm 56 [†]	185 \pm 90

* Data represent means \pm standard deviation of 13 neurons from NT brains and 20 neurons from T brains; cross-sectional data are from 11 neurons from NT brains and 14 neurons from T brains.

[†] Significant difference between T and NT ($P < 0.05$).

current steps that would increase the membrane potential by 20 mV based on input resistance. Percent accommodation was the percent increase in interspike interval for the last two spikes in a train compared with the first two spikes. The amount of "sag" in the voltage curve, which reflects rectification, was measured for 500 ms current steps, that caused hyperpolarization to approximately -80 and -100 mV and was the voltage change at the end of the step divided by the peak voltage change ($\times 100$).

Data Analyses

All data in the text are reported as means \pm standard deviation, and data in graphs are plotted as mean \pm standard error of the mean. Data from 27 cells (NT, 9; T, 18) from the slice preparation and six cells (NT, 4; T, 2) recorded in the whole brain preparation are included here. Statistical comparisons were performed using SPSS analysis software (SPSS, Chicago, IL). Data were analyzed using a two-way ANOVA with preparation (whole brain or slice) and social status (T or NT) as factors. There were few significant differences due to preparation (firing rate; see Results), so data from both preparations were pooled for reported means from T and NT males. A chi-square test was used to analyze categorical data.

RESULTS

Data reported here include 13 neurons from 10 NT males and 20 neurons from 16 T males. As expected from previous work, NT males had significantly smaller gonadosomatic indices than T males (NT, 0.23 ± 0.11 ; T, 0.57 ± 0.13 ; $F_{1,24} = 44.5$; $P < 0.0001$), confirming that their HPG axes were regressed [12, 13, 17]. In addition, the cross-sectional area of GnRH neurons was smaller in NT males than in T males (see Table 1; $F_{1,21} = 10.7$; $P < 0.01$), and this difference was independent of body size (ANCOVA with body length: $F_{1,20} = 7.9$; $P < 0.01$).

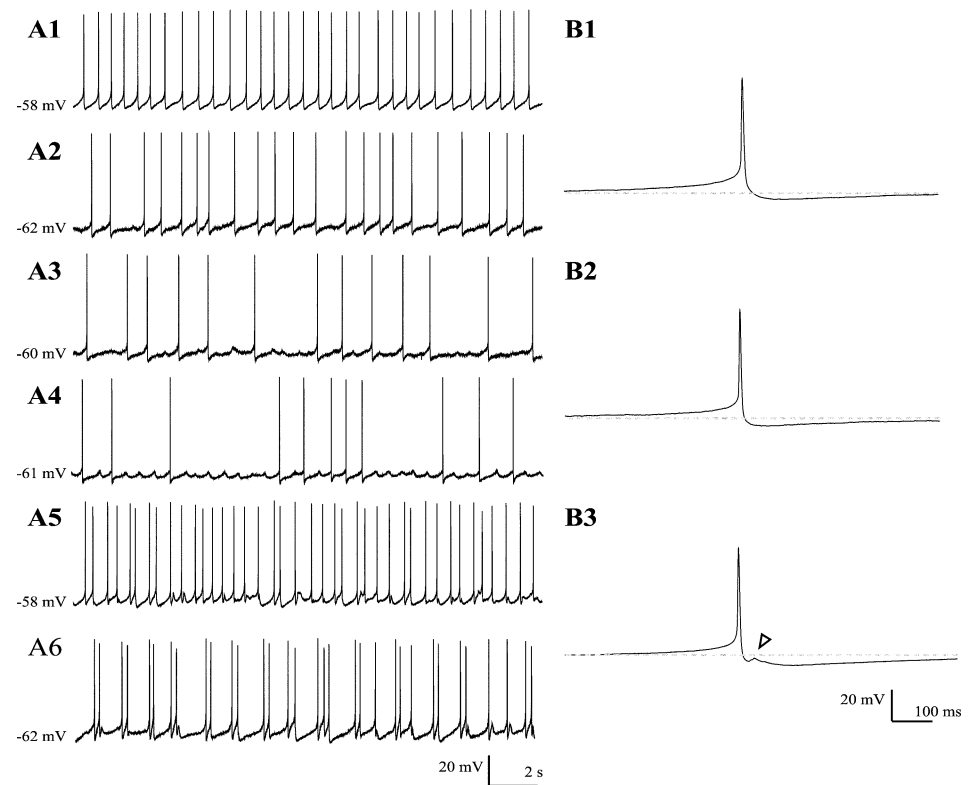
RMP and Spontaneous Firing Properties

The average RMP of all GnRH neurons was -60 ± 4 mV and did not differ in neurons from T and NT males (NT, -60 ± 4 mV; T, -60 ± 4 mV; $P > 0.5$).

In both T and NT males, most GnRH neurons were spontaneously active and exhibited one of several distinct firing patterns (see Fig. 2). Three neurons (NT, 2 of 13; T, 1 of 20) did not fire spontaneous action potentials for the entire recording session, up to 30 min, but did fire in response to positive current injection. Of spontaneously firing neurons, the majority displayed an irregular spiking pattern (NT, 9 of 11; T, 17 of 19), whereas the remainder showed regular spiking consisting of evenly spaced action potentials (NT, 2 of 11; T, 2 of 19). Some irregularly spiking neurons displayed semi-patterned activity consisting of clusters of action potentials (see Fig. 2, A5 and A6). These neurons are described in more detail below. The proportion of cells with different firing patterns did not differ as a function of reproductive status ($P > 0.4$). The type of firing pattern was not attributable to the resting membrane potential ($P > 0.5$).

Many neurons displayed oscillations in membrane po-

FIG. 2. Spontaneous activity patterns from representative GnRH neurons. Panels (A1–6) are each from a different neuron. A1) Voltage record from a neuron with a regular interspike interval. A2–4) Voltage record from three different neurons with irregular spontaneous firing patterns. A5–6) Firing patterns from neurons with a biphasic AHP. B1–3) Individual action potentials from the traces on the left at expanded time resolution. B1) Taken from trace A1. B2) Taken from trace A3. B3) Taken from trace A5 and shows a distinct biphasic or “notched” appearance; the notch is indicated by an arrowhead.



tential underlying the spontaneous generation of action potentials (see Fig. 2A4). Membrane oscillations were usually only apparent when they did not reach the threshold for action potential generation. These oscillations appeared to be intrinsically generated as judged by the fact that pulled-off patches retained the ability to exhibit oscillations (data not shown).

The initial spontaneous firing rate was quite variable across cells and both within and across individual animals and did not differ as a function of social status (T, 1.1 ± 1.2 Hz; NT, 2.2 ± 1.9 ; $P > 0.2$). However, there was a difference in initial spontaneous firing rate as a function of experimental preparation (slice vs. whole brain), with cells in the whole brain demonstrating significantly lower firing rates than cells recorded in slices (whole brain [$n = 6$], 0.45 ± 0.56 Hz; slice [$n = 27$], 1.76 ± 1.66 Hz; $F_{1,29} = 6.4$; $P < 0.02$).

Phasic Firing

Since GnRH neurons in mammals have been reported to exhibit episodic firing patterns [31, 32], we examined the spontaneous activity over long time periods (up to 30 min). Most neurons appeared to fire more or less continuously, with little change in average firing rate over time. However, a small fraction (3 of 20, 15%) of neurons from T males showed phasic activity patterns on a variety of timescales, with periods of silence from 10 sec to 3 min between firing episodes (Fig. 3). These neurons had membrane oscillations of approximately 5 mV underlying action potential generation. Since such neurons were encountered only rarely, they were not examined in detail.

Action Potential Properties

Typical action potential profiles are shown in Figure 2. In all neurons, action potentials were followed by an AHP.

In a subset of neurons from both T and NT males (NT, 4 of 13, 31%; T, 7 of 20, 35%), the AHP appeared distinctly biphasic or “notched” (see Fig. 2B3). Specifically, action potentials in such neurons appeared to be followed by a brief, fast AHP; a slight depolarization; and a second slow AHP (Fig. 2B3). Cells that displayed the notched AHP profile generated an interesting spontaneous firing pattern consisting of spikes clustered in doublets and occasionally triplets (see Fig. 2, A5 and A6).

Properties of spontaneously generated action potentials were analyzed and compared as a function of social status (Table 2). Action potentials recorded from neurons in NT males were significantly longer in duration than those recorded from T males ($F_{1,29} = 8.06$; $P < 0.01$; Table 2; Fig. 4). The difference in duration was not explainable by spike height (ANCOVA with action potential height, $F_{1,28} = 5.7$; $P < 0.02$). Action potential height and relative threshold were not significantly different as a function of reproductive state.

We investigated whether the difference in action potential duration as a function of reproductive state was characterized by differences in the depolarization or repolarization phase of the action potential. Although rise time was similar in neurons from T and NT males ($P > 0.5$), there was a significant difference in decay time ($F_{1,29} = 8.5$; $P < 0.01$). In addition, the AHP was reduced in neurons from NT males both in amplitude ($F_{1,19} = 9.6$; $P < 0.01$) and time to peak ($F_{1,19} = 11.3$; $P < 0.01$). Neurons that exhibited a biphasic AHP were not included in the analysis of AHP properties because their AHP was significantly different from nonnotched cells (data not shown).

Response to Negative Current Injection

GnRH neurons responded to increasingly negative current steps with approximately linear increases in voltage (see Fig. 5). The voltage response to negative 500 ms cur-

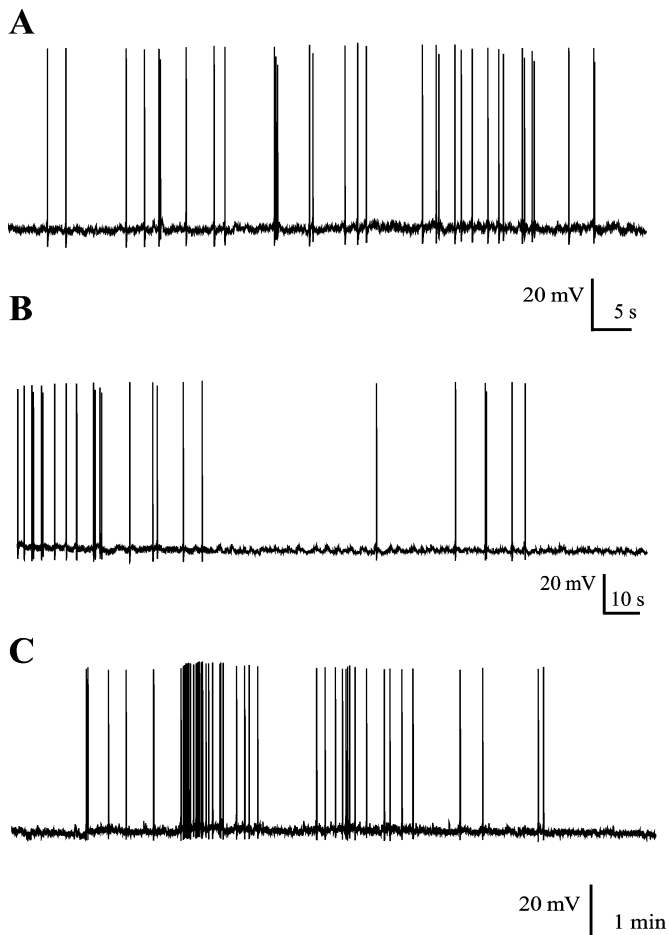


FIG. 3. Examples of episodic firing activity in neurons from territorial males. Traces shown in **A**, **B**, and **C** each depict different neurons that showed variations in firing rate over time. Each trace is a different time period, as noted in scale bars.

rent steps that caused a 20 mV change in membrane potential was used to calculate the total membrane capacitance and input resistance (see Fig. 5 and Table 1). Neurons from T males showed a smaller voltage change in response to the same magnitude current step when compared with neurons from NT males (i.e., they had a significantly lower input resistance; $F_{1,29} = 6.9$; $P < 0.02$; Table 1). In addition, neurons from T males had larger membrane capacitance on average than those from NT males (Table 1; $F_{1,29} = 11.2$; $P < 0.01$). These differences likely reflect the distinct average cell sizes of neurons from T and NT males (see above and Table 1). Capacitance and cell cross-sectional area were highly correlated (Fig. 6; $r = 0.676$; $P < 0.01$; $n = 25$). Cell input resistance is related to surface area and volume, as well as to currently active conductances; thus it is not simply linearly related to cross-sectional area. Nevertheless, cell size and input resistance were significantly correlated (Fig. 6; $r = -0.488$; $P = 0.013$; $n = 25$).

A subset of neurons displayed rebound excitation following hyperpolarization, reflected by the tendency to fire an action potential after a hyperpolarizing current step (e.g., Fig. 5A). The proportion displaying rebound action potentials did not differ as a function of reproductive status (NT, 7 of 13; T, 8 of 20; $P > 0.40$).

With steps to potentials below approximately -100 mV, a small amount of inward rectification was evident in volt-

TABLE 2. Action potential properties as a function of reproductive state.*

	Nonterritorial (NT) males	Territorial (T) males
Threshold relative to rest (mV)	11 ± 2.6	12 ± 3.0
AP height (mV)	72 ± 4	80 ± 8
AP duration (ms)	$3.3 \pm 0.7^\dagger$	2.7 ± 0.5
Rise time (ms)	1.08 ± 0.5	0.94 ± 0.4
Decay time (ms)	$2.14 \pm 0.5^\dagger$	1.7 ± 0.3
AHP relative to rest (mV)	$-4.6 \pm 1.6^\dagger$	-6.7 ± 0.7
Time to AHP peak (ms)	$45.8 \pm 18^\dagger$	23.8 ± 10

* Data represent means \pm standard deviation of 13 neurons from NT brains and 20 neurons from T brains; for AHP properties, sample size is 10 neurons from NT brains and 13 neurons from T brains. AP, action potential.

† Significant difference between T and NT ($P < 0.05$).

age traces from neurons from both T and NT males (data not shown). We compared the voltage change near the end of a 500 ms current pulse to the peak voltage change caused by a step to approximately -100 mV. For steps to -100 mV, the peak was $96.6\% \pm 1.8\%$ (T males, $n = 10$) or $96.8\% \pm 1.3\%$ (NT males, $n = 7$), whereas the rectification was less evident in steps to -80 mV, and the percent change was $99.0\% \pm 0.7\%$ (T males, $n = 16$) or $99.1\% \pm 0.8\%$ (NT males, $n = 13$).

Evoked Firing Properties

We presented neurons with 500 ms positive current steps to determine repetitive firing properties (Fig. 7). As described above, neurons from NT males had higher input resistance than those from T males. Therefore, in neurons from NT males the same magnitude of current injection caused a higher frequency of evoked spikes on average than those from T males (Fig. 7). To control for these differences in input resistance, we analyzed the evoked firing of neurons in response to a current change that would cause an approximately 20 mV change in membrane potential.

Fish GnRH neurons showed limited spike frequency accommodation: neurons fired more or less continuously in response to positive current injections (see Fig. 7). We de-

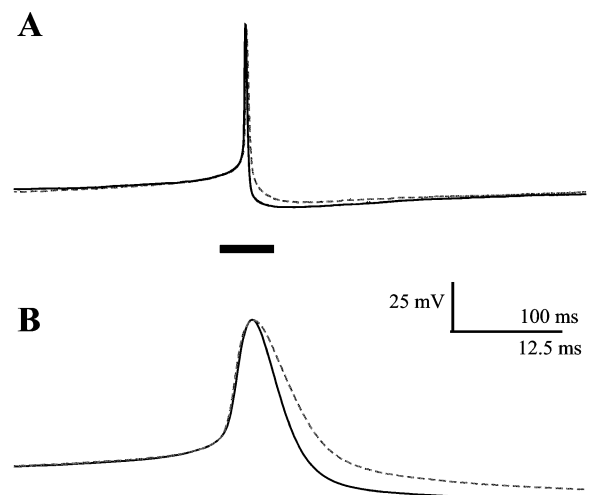


FIG. 4. Comparison of action potential shape as a function of reproductive status. **A**) Spikes from neurons from a T and an NT male are superimposed using the threshold to align the signals. The neuron recorded from a T male is depicted by a black solid line, and that from the NT male a grey dashed line. **B**) An expanded timescale from the trace in **A** corresponding to the time delineated by a bar.

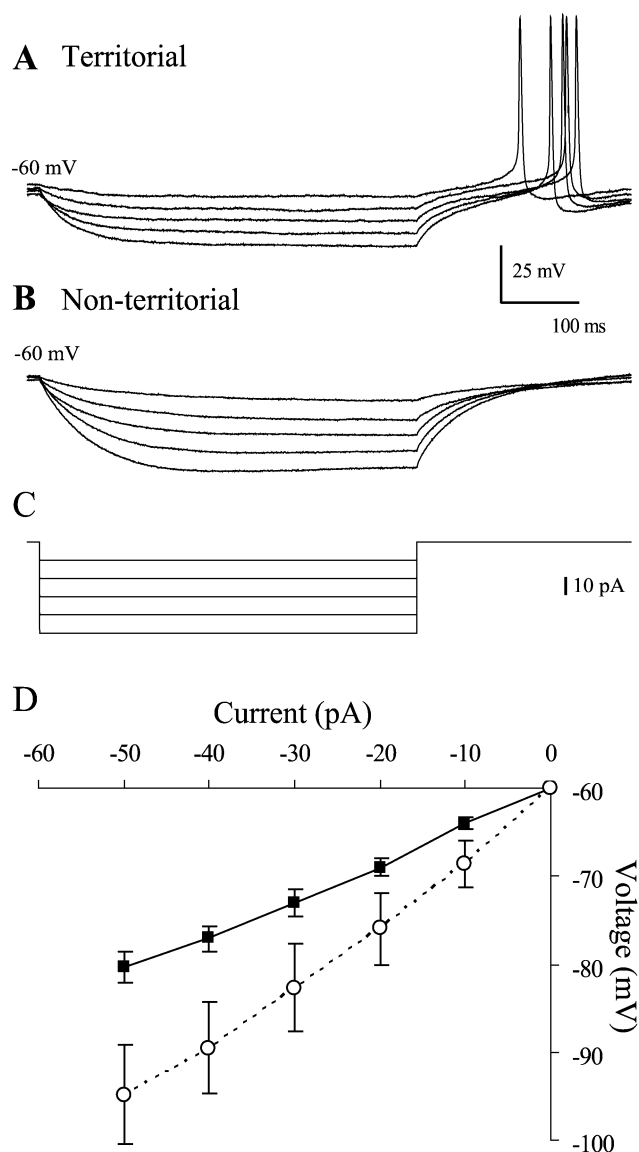


FIG. 5. Response of T and NT GnRH neurons to negative current injection. Both cells were injected with 500 ms negative current steps of 10 pA from -10 to -50 pA as shown in (C). **A**) Response to current injection for a neuron from a T male with an input resistance of 340 M Ω . **B**) Response to current injection for neuron from an NT male with an input resistance of 650 M Ω . These neurons had input resistances near the mean of their respective group (see Table 1). Note that this neuron from a T male showed a post-hyperpolarization rebound spike; however, the presence of such rebound depolarization was found equally often in neurons from T and NT males (see *Results*). **D**) Mean (\pm SEM) current-voltage relationship for the population of neurons from T and NT males presented with the above current steps. Neurons from T males are shown in filled squares ($n = 15$), and neurons from NT males are shown in unfilled circles ($n = 10$). The resting potential has been plotted as 0 current injection.

terminated the extent of accommodation by measuring the percent increase in the interspike interval across the spike train, which did not differ as a function of reproductive state: T ($n = 13$), $11\% \pm 3\%$; NT ($n = 8$), $13\% \pm 7\%$; $P > 0.5$.

We also compared the number of action potentials evoked by positive current injection and the time between spikes in these trains in neurons from T and NT males. There was a tendency for neurons from NT males to have

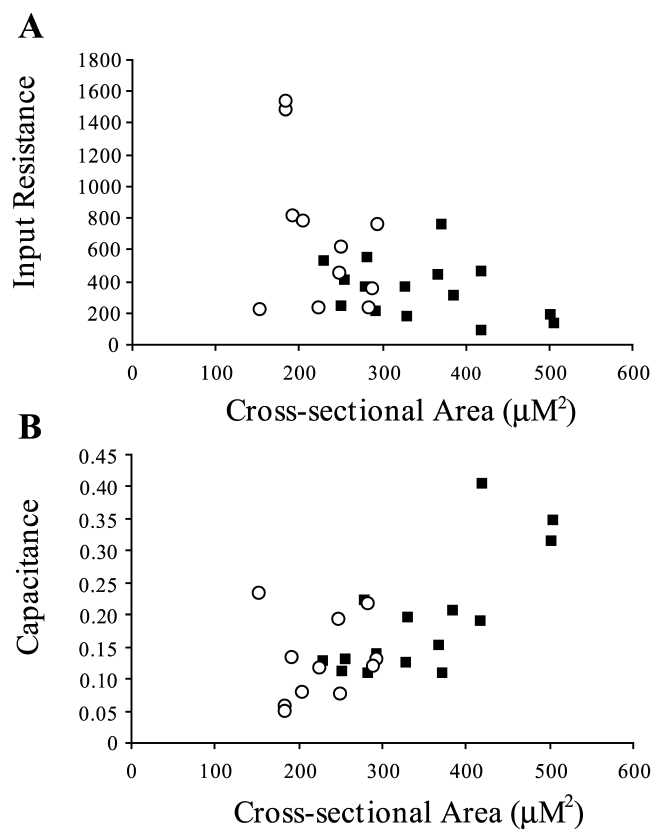


FIG. 6. Passive electrical properties as a function of cell size. Correlations between cell cross-sectional area and input resistance (**A**) or total membrane capacitance (**B**). Neurons from T males are shown in filled squares ($n = 14$), and neurons from NT males are shown in unfilled circles ($n = 11$).

a larger interspike interval (T [$n = 13$], 94 ± 4.4 ms; NT [$n = 8$], 104 ± 8.5 ms; $F_{1,19} = 2.62$; $P = 0.12$) and to fire fewer spikes (T [$n = 13$], 10 ± 0.55 Hz; NT [$n = 8$], 8.75 ± 0.75 Hz; $F_{1,19} = 1.85$; $P = 0.18$); however, these differences were not statistically significant.

DISCUSSION

This report provides the first electrophysiological characterization of hypothalamic GnRH neurons in any non-mammalian species. We compared the basic electrical properties as a function of reproductive state and identified several changes that corresponded to differences in fertility. Here, we will compare fish GnRH neurons with those from mammals and discuss potential implications of the electrical differences we observed between reproductive and non-reproductive males.

Comparison of Fish GnRH Neurons With Those of Mammals

A typical signature of the electrical activity of GnRH neurons has not yet emerged from electrophysiological experiments in mammals. Because GnRH and the gonadotropins are released episodically [33–37], it was predicted that the activity patterns of GnRH neurons might reflect this pulsatility. In fact, three different types of activity patterns have been described from *in vitro* recordings of adult mammalian GnRH neurons: 1) episodic activity at timescales similar to that of pulsatile release. One study reported that

71% of recorded neurons showed periods of quiescence up to 30 min between firing episodes [31], whereas another described modulation of firing rate on long timescales [32]; 2) episodic activity occurring on timescales much shorter than pulsatile release. Several reports describe a subset of GnRH cells that fire in bursts, or clusters of two or more spikes at intervals ranging from 1 to 10 sec [32; 27%, 38; 93%, 39]; and 3) continuous activity, or no description of phasic activity [22–24].

Since gonadotropins are also released episodically in fish [40–43], we examined whether the spontaneous activity of *A. burtoni* GnRH neurons showed any reflection of pulsatility. The activity patterns we recorded fell primarily into the last two categories described above: episodic activity on short timescales or continuous firing. Most fish GnRH neurons fired more or less continuously (see Fig. 2). A subset of neurons from T males (15%) exhibited evidence of phasic activity patterns (see Fig. 3); however, this phasic activity was not on timescales predicted to underlie reproductive hormone release in fish [41–43]. Some neurons had spikes with a biphasic AHP that caused an interesting pattern of activity consisting of clusters of spikes in doublets or occasionally triplets (see Fig. 2), a pattern reminiscent of high-frequency clustering activity described in mouse neurons [32, 38, 44].

Although we did not see many overt examples of episodic activity, most fish GnRH neurons exhibited electrical activity suggestive of a capacity for episodic firing. First, a subset of neurons exhibited a biphasic AHP (see Fig. 2), consisting in part of a slow AHP, which resembled a slow AHP mediated by a calcium-activated potassium current [45, 46]. Calcium-activated potassium currents are known to regulate aspects of episodic firing in some neurons [45]. However, we did not see spike-frequency adaptation (see Fig. 7), which is often associated with the presence of a type of calcium-activated potassium channel (SK channels) [46]. Thus, whether calcium-activated potassium currents are present (and which types) in fish GnRH neurons remains to be determined. Whatever the cause, neurons with a biphasic AHP exhibited an interesting episodic firing pattern (see Fig. 2). Second, a subset of neurons demonstrated rebound depolarization following hyperpolarization (see Fig. 5). This type of activity can be generated by T- or H-currents, which are involved in burst generation and have been identified in mammalian GnRH neurons [23, 47–49]. Finally, most neurons showed membrane oscillations (see Fig. 2) similar to those described in mouse GnRH neurons, which are thought to be important in generating high-frequency bursts [38, 44]. In addition, membrane oscillations are critical to pacemaking in nonhypothalamic GnRH neurons recorded from the terminal nerve of fish [26].

Variation of Electrical Properties With Reproductive State

We identified a difference in action potential repolarization in GnRH neurons as a function of reproductive capacity. Action potential duration was longer in neurons from NT males, which are reproductively regressed, and their AHP was delayed and less negative when compared with neurons from T males, which are reproductively active (see Fig. 4). A less substantial AHP in neurons from NT males would remove inactivation from fewer numbers of potassium and sodium channels, which would lead to an increased time to the next spike. Indeed, neurons from NT males tended to have longer interspike intervals during evoked firing episodes. The lesser AHP and longer duration

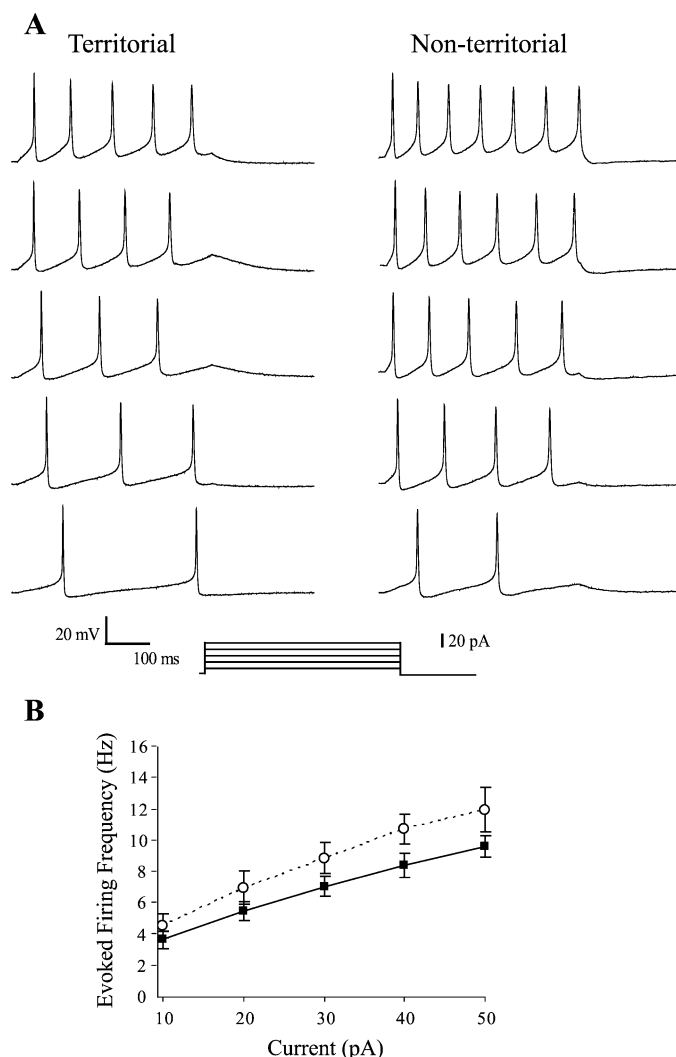


FIG. 7. Evoked firing properties. **A**) The response of typical neurons from T and NT males to increasing 500 ms current pulses from +10 to +50 pA is shown from bottom to top. The input resistance was 430 M Ω for the neuron from a T male and 750 M Ω for the neuron from an NT male. **B**) Mean (\pm SEM) frequency of spikes evoked by a 500 ms current injection for all neurons from T and NT males presented with the above range of current pulses. Neurons from T males are shown in filled squares ($n = 12$), and those from NT males are shown in unfilled circles ($n = 10$).

action potential in neurons from NT males could thus serve to limit their maximum firing rate. In many types of neuroendocrine cells, secretion is achieved by bursts of action potentials, which synergistically increase the efficacy of release [50–55]. If bursts play a similar role in GnRH neurons, a limited maximum firing rate in neurons from NT males would likely decrease the efficiency of GnRH release and cause a decreased amount of GnRH released per burst.

We found that action potential decay, but not rise, characteristics differed in neurons from T and NT males. This, together with evidence of a reduced AHP, leads us to hypothesize that this difference is due to changes in a potassium conductance, because potassium generally mediates action potential repolarization and the AHP [45]. We have not investigated what specific potassium conductance might underlie the differences in action potential repolarization in fish GnRH neurons; however, several types of potassium channels have been described in GnRH neurons from female mice and guinea pigs, including A-type [23, 56]; de-

laid rectifier [23, 56]; and inwardly rectifying potassium channels [23, 57]. Some of these potassium channels have been identified as a target of steroid hormone modulation [56, 58]. This is of particular interest because T and NT males have differences in circulating levels of sex steroids and stress hormones [19, 59]. Previous work has shown that androgens influence GnRH cell size in T males [19]. Additionally, cortisol has been proposed as a mediator of reproductive differences in *A. burtoni*, because NT males have higher levels of cortisol than T males [59]. It will be interesting to determine which types of potassium channel(s) might be regulated as a function of reproductive state in *A. burtoni* and if they are modulated by steroid hormones such as testosterone and cortisol.

Other electrical properties that varied with reproductive state were changes in input resistance and membrane capacitance. These differences were related to distinct average cell sizes in T and NT males. Specifically, larger neurons from T males had larger membrane capacitance and lower input resistance compared with smaller neurons from NT males. The reason for changes in cell size in these two populations is not clear. However, changes in cell size have been noted in other neuroendocrine systems in both fish [60–62] and mammals [63], and cell hypertrophy is a common feature of peripheral endocrine systems (e.g., thyroid and adrenal glands). It may be that there are restrictions on synthesis and packaging as a function of size for such secretory cells. Whatever the cause, changes in cell size have important consequences for an excitable cell. Specifically, for a given synaptic input, neurons in T males that have lower input resistance and larger capacitance will be more difficult to influence electrically, and thus will tend to be more electrically isolated. Future work in *A. burtoni* may consider the impact of differences in capacitance and input resistance on the efficacy of synaptic communication and the response to neurotransmitter application as a function of reproductive state to determine whether GnRH neurons in T males are indeed more electrically isolated. If so, and if this translates into physiology *in vivo*, how can this be reconciled with the clear evidence of functional upregulation in the HPG axis downstream of GnRH neurons in T males? One possible explanation is that an ongoing rhythm that was intrinsically generated would be less likely to be affected by synaptic influences in these larger neurons. Therefore, if GnRH pulsatility was generated endogenously within GnRH neurons, reducing the impact of external synaptic influences may be an advantageous by-product of increasing cell size. The question of whether GnRH pulsatility is an endogenous property of GnRH neurons has intrigued GnRH neurobiologists since the earliest inquiries into the GnRH system [reviewed in 20], and recent work in the mouse has begun to elucidate that aspects of pulsatility may indeed be generated endogenously [reviewed in 44].

Aside from changes in action potential properties and electrical properties related to cell size, most electrical characteristics of GnRH neurons from T and NT males were maintained despite dramatic differences in reproductive capacity between these male types. For instance, there were no obvious changes in spontaneous firing rates or patterns as a function of reproductive state. Because our recordings were performed *in vitro* and therefore outside of the normal hormonal milieu, which differs between T and NT males, some of this lack of difference may be attributable to hormonal differences that exist *in vivo* that were not replicated in our experimental preparation. Additionally, as in any

whole-cell recording paradigm, important intracellular components may have been washed away during recording, which is a concern because G-protein cascades are thought to be an important player in the generation of GnRH pulsatility in mice [44, 64]. Despite these caveats, however, it is likely that some of the electrical similarities we described as a function of reproductive state are a true reflection of GnRH biology. For example, GnRH neurons showing activity suggestive of the presence of conductances involved in episodic firing were found equally in T and NT brains. In concordance with these results, evidence suggests that the modulation of the GnRH system during reproductive transitions is not achieved by the differential expression of pulsatility, but instead the frequency of pulses, and in some cases pulse amplitude, is varied [65, 66]. Similar changes in hormone patterns have also been reported across reproductive cycles in fish [42, 43]. Therefore, because the pulsatile nature of the activity is not predicted to change, the underlying conductances should remain fundamentally similar as a function of reproductive state. Accordingly, results from mice are similar to those we report from fish: there are few differences in GnRH neuron electrophysiology across the estrous cycle of mice, with a notable exception of action potential duration [23].

In summary, this work has provided the first electrical characterization of GnRH neurons in a male animal across reproductive states and in any nonmammalian species. GnRH neurons are essential for reproduction in all vertebrates, and the conservation or divergence of their electrical properties revealed by a comparative analysis will provide important insight into their function. For instance, our results suggest that fish are similar to mammals in that few changes in the basic electrical properties are noted in different reproductive states. This is an important contribution to the emerging story about the function of these vital neuroendocrine cells.

ACKNOWLEDGMENTS

We thank M. Finley, J. Huguenard, and D. Madison for technical advice, and S. Moenter, S. Burmeister, K. Hoke, R. Henderson, K. Grens, M. Scanlon, and three anonymous reviewers for useful comments on earlier drafts of this manuscript.

REFERENCES

- Ortius D, Heinze J. Fertility signaling in queens of a North American ant. *Behav Ecol Sociobiol* 1999; 45:151–159.
- Stern K, McClintock MK. Regulation of ovulation by human pheromones. *Nature* 1998; 392:177–179.
- Cheng MF, Peng JP, Johnson P. Hypothalamic neurons preferentially respond to female nest coo stimulation: demonstration of direct acoustic stimulation of luteinizing hormone release. *J Neurosci* 1998; 18:5477–5489.
- Faulkes CG, Abbott DH. Social control of reproduction in breeding and non-breeding male naked mole-rats (*Heterocephalus glaber*). *J Reprod Fertil* 1991; 93:427–435.
- McComb K. Roaring by red deer stags advances the date of oestrus in hinds. *Nature* 1987; 330:648–649.
- Ojeda SR, Prevot V, Heger S, Lomniczi A, Dziedzic B, Mungenast A. Glia-to-neuron signaling and the neuroendocrine control of female puberty. *Ann Med* 2003; 35:244–255.
- Terasawa E, Fernandez DL. Neurobiological mechanisms of the onset of puberty in primates. *Endocr Rev* 2001; 22:111–151.
- Herbison AE. Multimodal influence of estrogen upon gonadotropin-releasing hormone neurons. *Endocr Rev* 1998; 19:302–330.
- Lehman MN, Goodman RL, Karsch FJ, Jackson GL, Berriman SJ, Jansen HT. The GnRH system of seasonal breeders: anatomy and plasticity. *Brain Res Bull* 1997; 44:445–457.
- Bakker J, Baum MJ. Neuroendocrine regulation of GnRH release in induced ovulators. *Front Neuroendocrinol* 2000; 21:220–262.

11. Rissman EF. Behavioral regulation of gonadotropin-releasing hormone. *Biol Reprod* 1996; 54:413–419.
12. Davis MR, Fernald RD. Social control of neuronal soma size. *J Neurobiol* 1990; 21:1180–1188.
13. Francis RC, Soma K, Fernald RD. Social regulation of the brain-pituitary-gonadal axis. *Proc Natl Acad Sci U S A* 1993; 90:7794–7798.
14. White SA, Nguyen T, Fernald RD. Social regulation of gonadotropin-releasing hormone. *J Exp Biol* 2002; 205:2567–2581.
15. Fernald RD, Hirata NR. Field study of *Haplochromis burtoni*: quantitative behavioural observations. *Anim Behav* 1977; 1977:964–975.
16. Fernald RD. Quantitative behavioural observations of *Haplochromis burtoni* under semi-natural conditions. *Anim Behav* 1977; 25:643–653.
17. Fraley NB, Fernald RD. Social control of developmental rate in the African cichlid, *Haplochromis burtoni*. *Z Tierpsychol* 1982; 60:66–82.
18. Hofmann HA, Benson ME, Fernald RD. Social status regulates growth rate: consequences for life-history strategies. *Proc Natl Acad Sci U S A* 1999; 96:14171–14176.
19. Soma KK, Francis RC, Wingfield JC, Fernald RD. Androgen regulation of hypothalamic neurons containing gonadotropin-releasing hormone in a cichlid fish: integration with social cues. *Horm Behav* 1996; 30:216–226.
20. Knobil E. The GnRH pulse generator. *Am J Obstet Gynecol* 1990; 163:1721–1727.
21. Stern JE, Armstrong WE. Changes in the electrical properties of supraoptic nucleus oxytocin and vasopressin neurons during lactation. *J Neurosci* 1996; 16:4861–4871.
22. Kelly MJ, Ronnekleiv OK, Eskay RL. Identification of estrogen-responsive LHRH neurons in the guinea pig hypothalamus. *Brain Res Bull* 1984; 12:399–407.
23. Sim JA, Skynner MJ, Herbison AE. Heterogeneity in the basic membrane properties of postnatal gonadotropin-releasing hormone neurons in the mouse. *J Neurosci* 2001; 21:1067–1075.
24. Spergel DJ, Kruth U, Hanley DF, Sprengel R, Seeburg PH. GABA- and glutamate-activated channels in green fluorescent protein-tagged gonadotropin-releasing hormone neurons in transgenic mice. *J Neurosci* 1999; 19:2037–2050.
25. Suter KJ, Song WJ, Sampson TL, Wuarin JP, Saunders JT, Dudek FE, Moenter SM. Genetic targeting of green fluorescent protein to gonadotropin-releasing hormone neurons: characterization of whole-cell electrophysiological properties and morphology. *Endocrinology* 2000; 141:412–419.
26. Oka Y, Matsushima T. Gonadotropin-releasing hormone (GnRH)-immunoreactive terminal nerve cells have intrinsic rhythmicity and project widely in the brain. *J Neurosci* 1993; 13:2161–2176.
27. Oka Y. Physiology and release activity of GnRH neurons. *Prog Brain Res* 2002; 141:259–281.
28. Mittman S, Flaming DG, Copenhagen DR, Belgum JH. Bubble pressure measurement of micropipet tip outer diameter. *J Neurosci Methods* 1987; 22:161–166.
29. Fernald RD, Shelton LC. The organization of the diencephalon and the preteectum in the cichlid fish, *Haplochromis burtoni*. *J Comp Neurol* 1985; 238:202–217.
30. Silverman AJ. The gonadotropin-releasing hormone (GnRH) neuronal systems: immunocytochemistry. In: Knobil E, Neill JD (eds.), *The Physiology of Reproduction*. New York: Raven Press; 1988:1283–1304.
31. Suter KJ, Wuarin JP, Smith BN, Dudek FE, Moenter SM. Whole-cell recordings from preoptic/hypothalamic slices reveal burst firing in gonadotropin-releasing hormone neurons identified with green fluorescent protein in transgenic mice. *Endocrinology* 2000; 141:3731–3736.
32. Nunemaker CS, Straume M, DeFazio RA, Moenter SM. Gonadotropin-releasing hormone neurons generate interacting rhythms in multiple time domains. *Endocrinology* 2003; 144:823–831.
33. Carmel PW, Araki S, Ferin M. Pituitary stalk portal blood collection in rhesus monkeys: evidence for pulsatile release of gonadotropin-releasing hormone (GnRH). *Endocrinology* 1976; 99:243–248.
34. Dierschke DJ, Bhattacharya AN, Atkinson LE, Knobil E. Circoral oscillations of plasma LH levels in the ovariectomized rhesus monkey. *Endocrinology* 1970; 87:850–853.
35. Foster DL, Lemons JA, Jaffe RB, Niswender GD. Sequential patterns of circulating luteinizing hormone and follicle-stimulating hormone in female sheep from early postnatal life through the first estrous cycles. *Endocrinology* 1975; 97:985–994.
36. Gay VL, Sheth NA. Evidence for a periodic release of LH in castrated male and female rats. *Endocrinology* 1972; 90:158–162.
37. Levine JE, Pau KY, Ramirez VD, Jackson GL. Simultaneous measurement of luteinizing hormone-releasing hormone and luteinizing hormone release in unanesthetized, ovariectomized sheep. *Endocrinology* 1982; 111:1449–1455.
38. Kuehl-Kovarik MC, Pouliot WA, Halterman GL, Handa RJ, Dudek FE, Partin KM. Episodic bursting activity and response to excitatory amino acids in acutely dissociated gonadotropin-releasing hormone neurons genetically targeted with green fluorescent protein. *J Neurosci* 2002; 22:2313–2322.
39. Nunemaker CS, DeFazio RA, Moenter SM. Estradiol-sensitive afferents modulate long-term episodic firing patterns of GnRH neurons. *Endocrinology* 2002; 143:2284–2292.
40. Habibi HR. Homologous desensitization of gonadotropin-releasing hormone (GnRH) receptors in the goldfish pituitary: effects of native GnRH peptides and a synthetic GnRH antagonist. *Biol Reprod* 1991; 44:275–283.
41. Hontela A, Peter RE. Daily cycles in serum gonadotropin levels in the goldfish: effects of photoperiod, temperature, and sexual condition. *Can J Zool* 1978; 56:2430–2442.
42. Zohar Y, Breton B, Fostier A. Short-term profiles of plasma gonadotropin and estradiol-17 beta levels in the female rainbow trout, from early ovarian recrudescence and throughout vitellogenesis. *Gen Comp Endocrinol* 1986; 64:172–188.
43. Zohar Y, Breton B, Fostier A. Short-term profiles of plasma gonadotropin and 17 alpha-hydroxy, 20 beta-dihydroprogesterone levels in the female rainbow trout at the periovulatory period. *Gen Comp Endocrinol* 1986; 64:189–198.
44. Moenter SM, DeFazio AR, Pitts GR, Nunemaker CS. Mechanisms underlying episodic gonadotropin-releasing hormone secretion. *Front Neuroendocrinol* 2003; 24:79–93.
45. Hille B. *Ion Channels of Excitable Membranes*. Sunderland, MA: Sinauer Associates; 2001.
46. Sah P. Ca(2+)-activated K+ currents in neurones: types, physiological roles and modulation. *Trends Neurosci* 1996; 19:150–154.
47. Kelly MJ, Wagner EJ. GnRH neurons and episodic bursting activity. *Trends Endocrinol Metab* 2002; 13:409–410.
48. Takagi H, Moenter SM. Hyperpolarization-activated currents in gonadotropin-releasing hormone (GnRH) neurons. In: *Online 2003 Abstract Viewer/Itinerary Planner*. Washington, DC: Society for Neuroscience; 2003: Program No. 611.11.
49. Kato M, Ui-Tei K, Watanabe M, Sakuma Y. Characterization of voltage-gated calcium currents in gonadotropin-releasing hormone neurons tagged with green fluorescent protein in rats. *Endocrinology* 2003; 144:5118–5125.
50. Bicknell RJ. Optimizing release from peptide hormone secretory nerve terminals. *J Exp Biol* 1988; 139:51–65.
51. Dutton A, Dyball RE. Phasic firing enhances vasopressin release from the rat neurohypophysis. *J Physiol* 1979; 290:433–440.
52. Dyball RE, Grossmann R, Leng G, Shibuki K. Spike propagation and conduction failure in the rat neural lobe. *J Physiol* 1988; 401:241–256.
53. Jackson MB, Konnerth A, Augustine GJ. Action potential broadening and frequency-dependent facilitation of calcium signals in pituitary nerve terminals. *Proc Natl Acad Sci U S A* 1991; 88:380–384.
54. Leng G, Brown D. The origins and significance of pulsatility in hormone secretion from the pituitary. *J Neuroendocrinol* 1997; 9:493–513.
55. Leng G, Dyball RE, Luckman SM. Mechanisms of vasopressin secretion. *Horm Res* 1992; 37:33–38.
56. DeFazio RA, Moenter SM. Estradiol feedback alters potassium currents and firing properties of gonadotropin-releasing hormone neurons. *Mol Endocrinol* 2002; 16:2255–2265.
57. Lagrange AH, Ronnekleiv OK, Kelly MJ. Estradiol-17 beta and mu-opioid peptides rapidly hyperpolarize GnRH neurons: a cellular mechanism of negative feedback? *Endocrinology* 1995; 136:2341–2344.
58. Kelly MJ, Qiu J, Wagner EJ, Ronnekleiv OK. Rapid effects of estrogen on G protein-coupled receptor activation of potassium channels in the central nervous system (CNS). *J Steroid Biochem Mol Biol* 2002; 83:187–193.
59. Fox HE, White SA, Kao MH, Fernald RD. Stress and dominance in a social fish. *J Neurosci* 1997; 17:6463–6469.
60. Olivereau M, Olivereau J. Effect of pharmacological adrenalectomy on corticotropin-releasing factor-like and arginine vasotocin immunoreactivities in the brain and pituitary of the eel: immunocytochemical study. *Gen Comp Endocrinol* 1990; 80:199–215.

61. Hofmann HA, Fernald RD. Social status controls somatostatin neuron size and growth. *J Neurosci* 2000; 20:4740–4744.
62. Semsar K, Godwin J. Social influences on the arginine vasotocin system are independent of gonads in a sex-changing fish. *J Neurosci* 2003; 23:4386–4393.
63. Stern JE, Armstrong WE. Reorganization of the dendritic trees of oxytocin and vasopressin neurons of the rat supraoptic nucleus during lactation. *J Neurosci* 1998; 18:841–853.
64. Krsmanovic LZ, Mores N, Navarro CE, Arora KK, Catt KJ. An agonist-induced switch in G protein coupling of the gonadotropin-releasing hormone receptor regulates pulsatile neuropeptide secretion. *Proc Natl Acad Sci U S A* 2003; 100:2969–2974.
65. Levine JE, Chappell P, Besecke LM, Bauer-Dantoin AC, Wolfe AM, Porkka-Heiskanen T, Urban JH. Amplitude and frequency modulation of pulsatile luteinizing hormone-releasing hormone release. *Cell Mol Neurobiol* 1995; 15:117–139.
66. Thiery JC, Martin GB. Neurophysiological control of the secretion of gonadotrophin-releasing hormone and luteinizing hormone in the sheep—a review. *Reprod Fertil Dev* 1991; 3:137–173.